Sensors and Actuators B 240 (2017) 1099–1105

Contents lists available at ScienceDirect

Sensors and Actuators B: Chemical

journal homepage: www.elsevier.com/locate/snb

Highly selective detection of dimethyl methylphosphonate (DMMP) using CuO nanoparticles /ZnO flowers heterojunction

Ran Yoo, Somi Yoo, Dongmei Lee, Jeongmin Kim, Sungmee Cho*, Wooyoung Lee*

Department of Materials Science and Engineering, Yonsei University, 262 Seongsanno Seodaemun-gu, Seoul, 129-749, South Korea

ARTICLE INFO

Article history:
Received 31 May 2016
Received in revised form 22 July 2016
Accepted 6 September 2016
Available online 8 September 2016

Keywords:
CuO NPs/ZnO flowers
Hydrothermal synthesis
Dimethyl methylphosphonate (DMMP) gas
Gas sensor

ABSTRACT

Here we report the fabrication of high surface area CuO nanoparticles (NPs) on micron-scale ZnO (CuO/ZnO) "flowers" with dimethyl methylphosphonate (DMMP) gas sensing capabilities. The formation of CuO NPs/ZnO heterojunction structures was confirmed by PXRD and TEM analyses. The gas sensing properties of the CuO NPs/ZnO structures showed a faster response time (26.2 s) compared to the exclusively ZnO-based sensor (330 s). The heterojunction sensors demonstrated the highest selectivity in 10 ppm DMMP, reaching the high value of 626.21 at 350 °C. This CuO NPs/ZnO heterojunction structure provides an extension of the depletion layer and an increase of the resistance (R_a) in air, leading to a reduction of the depletion layer and resistance (R_g) when exposed to reducing DMMP gas. The higher surface area (6.0 m^2/g) of the CuO/ZnO heterojunction structure with a 0.5 h synthesis time of the ZnO flowers further promoted the adsorption kinetics for the reaction between $C_3H_9O_3P$ and O^{2-} when exposed to DMMP, thus enhancing its sensing properties.

1. Introduction

The chemical warfare agents (CWAs) Sarin and Soman are some of the best-known chemical-based weapons of mass destruction. Sarin is a particularly dangerous gas since it causes severe effects on the human health system that can lead to neuromuscular paralysis or death while being both colorless and odorless [1,2]. Dimethyl-methyl-phosphonate (DMMP) is often studied as a simulant of Sarin. Several efforts have been attempted to detect the DMMP gas using semiconducting metal oxide (SMO) sensors because of their high sensitivity and simple methods of synthetic production [3–6]. More recently, DMMP gas sensors of other types, such as microcantilever (MCL) [7,8], quartz crystal microbalance (QCM) [9,10], and surface acoustic wave (SAW) [11,12] sensors, have introduced for improving sensing capabilities.

Among the many SMO materials available [13–15], ZnO is widely used in n-type semiconductors with a large bandgap value (E_g = 3.3 eV) owing to its high chemical stability, high sensitivity, short response time, and low cost [16–18]. CuO is another semiconductor that is widely used in sensor applications, however, unlike ZnO, CuO is a narrow bandgap (E_g = 1.2 eV) p-type semiconductor [17–22]. Technologies that combine these SMOs to form hybrid ZnO/CuO materials have been receiving increasing attention since the formation of the p/n junctions not only change energy structure of ZnO by occurring charge transfer, but also support the surface catalytic decomposition of other target gases in CuO [18,22]. Finally, this p/n junction can extend a depletion layer through interfacial electron-transfer processes in air, thus improving their sensing properties in the presence of the reducing gases (e.g., DMMP). Few studies have been conducted to develop CuO/ZnO based sensors for H_2S, H_2, and CO_2 detection [23–28]. Recently, several CuO/ZnO mixed metal oxide nanostructures with high surface-to-volume ratios or surface modifications, such as nanorods [29], nanocomposites [30], nanofibers [31], and core-shell [32], have been reported to show enhanced sensing capabilities. The ability of these CuO/ZnO heterojunction structures to detect DMMP gas has not yet been explored.

In this work, we report the microstructural evolution and DMMP gas sensing properties of CuO nanoparticles on micron-scale ZnO (CuO/ZnO) "flower" structures synthesized via a hydrothermal method. Based on our previous report, Al-doped-ZnO-based sensors showed improved sensing capabilities for the DMMP gas detection, i.e., surface modification with Al metal doping could increase O_2 vacancies and surface reactions, which could lead to decreased recovery and response times [33,34]. In this context,

* Corresponding authors.
E-mail addresses: wooyoung@yonsei.ac.kr (W. Lee), csmise@yonsei.ac.kr (S. Cho).

http://dx.doi.org/10.1016/j.snb.2016.09.028
0925-4005/

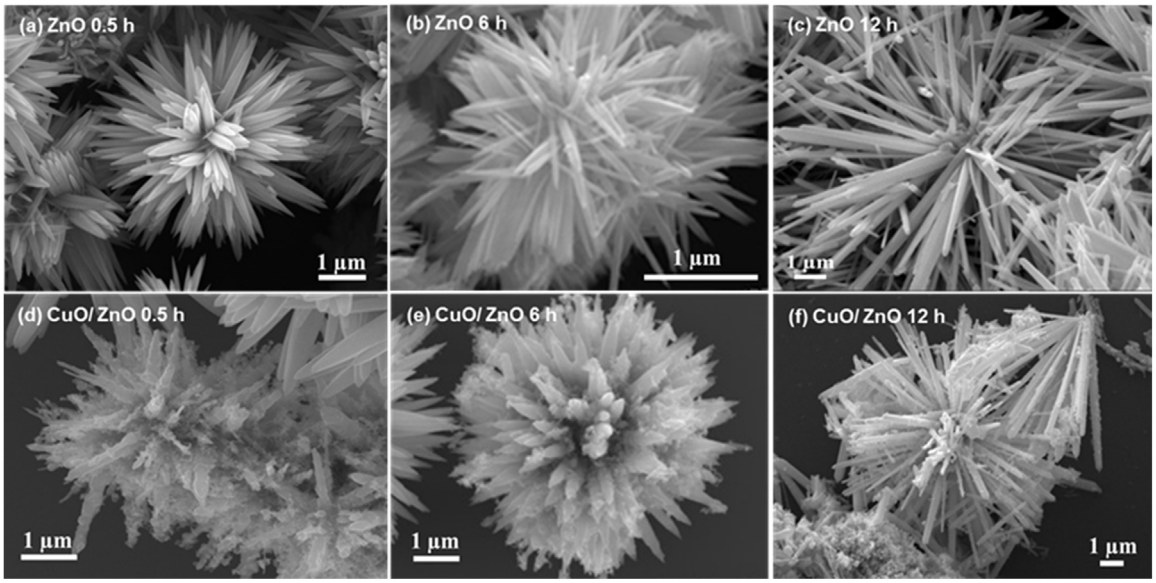

Fig. 1. Plane-view scanning electron microscopy (SEM) images of the surface morphology of both (a–c) ZnO and (d–f) ZnO/CuO structures as a function of ZnO synthesis time.

adding another p-type semiconductor like CuO nano particles (NPs) onto the ZnO flower structures after DMMP exposure could provide enhanced adsorption kinetics and reduce the thickness of the depletion layer in *p-n* junctions, thus improving *p*-CuO/*n*-ZnO sensor performance.

2. Experiment

2.1. Fabrication of ZnO and CuO NPs/ZnO based sensors

The synthesis of ZnO flowers was carried out via a hydrothermal method [29]. Zinc acetate dihydrate (0.5 M, Reagent Grade ≥98%, Sigma-Aldrich) and sodium hydroxide (5 M, Reagent Grade ≥98%, Sigma-Aldrich) were each dissolved in distilled water under constant stirring. The solutions were mixed, diluted with an additional 34 mL distilled water, and transferred to an autoclave. The Teflon-lined stainless steel autoclave was heated in an oven at 120 °C for 0.5, 6, and 12 h. After heating the solid product was collected by centrifugation, washed with methanol several times, air dried at 80 °C for 12 h, and then annealed at 400 °C for 2 h in air. For making the ZnO/CuO heterojunction structures, the resultant ZnO powders were suspended in ethanol and copper nitrate (0.25 wt%, Reagent Grade ≥98%, Sigma-Aldrich) was added with constant stirring. The mixtures were then air dried at 80 °C for 12 h and annealed at 400 °C for 2 h in air. To fabricate the CuO/ZnO hybrid sensor, both Ti (5 nm) and Pt (150 nm) electrode layers were deposited on a SiO_2 substrate through a DC magnetic sputtering process which was patterned by photolithography. The interdigitated Pt electrodes were 10 mm wide and 10 mm long, and spaced 10 μm. The synthesized CuO/ZnO powder was blended with α-terpinol binder and a small ink droplet 10 μL is placed on the interdigitated Pt electrode using a micropipette. Finally, the sample was heated at 300 °C for 1 h to remove the α-terpinol and annealed at 600 °C for 1 h.

2.2. Characterization

Structural data were collected using powder X-ray diffraction with Cu Kα1 radiation (λ = 0.15406 nm) (PXRD, Ultima IV/ME 200DX, Rigaku,), field-emission scanning electron microscopy (FE-SEM; JEOL 7001F equipped with an energy dispersive spectroscope), and transmission electron microscopy (TEM, JEOL JEM ARM 200F) with energy dispersive X-ray (EDX, X Max Oxford). The surface areas of the ZnO/CuO hybride flowers as a function of the ZnO synthesis time were measured by a Brunauer-Emmet-Teller (BET, Autosorb-iQ 2ST/MP) method employing a N_2 adsorption at 77 K after each sample was treated at 300 °C for 4 h under 10^{-4} Pa, using a Tristar-300 apparatus.

2.3. Gas-sensing properties

The electrical properties of the sensor mounted on a printed circuit board (PCB) were measured at 300–400 °C using a gas sensing system comprising a furnace (Korea Vacuum Tech., Korea), mass flow controllers (MFCs) for air, DMMP gas, cylinders of the target and air gases, a current source (Keithley 6220), and a nanovoltmeter (Keithley 2182). The sample was placed on a quartz cylinder in the furnace, and its signals were obtained from two Pt probes connected to the current source and the voltmeter, respectively. The DMMP gas concentration in the synthetic air was achieved by controlling its partial pressure by using MFCs. All the gas-sensing measurements were conducted on five samples in each concentrations at an operating temperature of 300–400 °C.

3. Results and discussion

3.1. Characterization of ZnO and CuO/ZnO materials

Fig. 1 shows plane-view scanning electron microscopy (SEM) images of the surface morphologies of both ZnO and CuO/ZnO as a function of ZnO synthesis time. As shown in Fig. 1(a)–(c), flower-shaped ZnO structures were formed and the size of the ZnO flower increased from approximately ~3–5–10 μm in diameter with increasing ZnO synthesis times. After mixing with CuO in the ZnO flowers, CuO nanoparticles were uniformly deposited on the surface of the ZnO flowers, as observed in Fig. 1(d)–(f). The BET surface area results showed that the surface area of the CuO nanoparticles deposited on the ZnO flowers decreased with increasing ZnO flower synthesis times, as shown in Fig. 2.

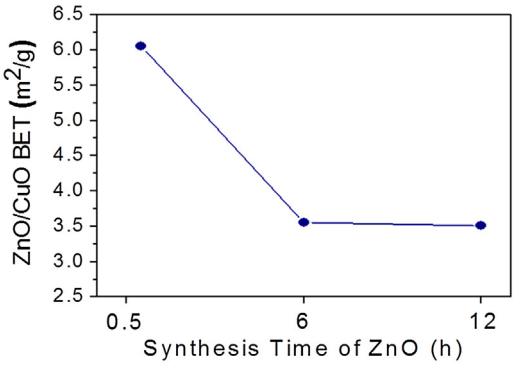

Fig. 2. Brunauer-Emmet-Teller (BET) surface area of *p*-CuO/*n*-ZnO vs. different synthesis time of ZnO (0.5, 6, and 12 h).

ZnO and CuO/ZnO samples with different ZnO synthesis times were characterized by powder X-ray diffraction (PXRD) as shown in Fig. 3. The main diffraction peaks of the ZnO flowers exhibits (100), (002), and (101) orientations which correspond to hexagonal wurtzite phase of ZnO (JCPDS # 36-1451), as shown in Fig. 3(a). In the CuO/ZnO structures with different ZnO synthesis times in Fig. 3(b)–(d), the PXRD patterns matched a monoclinic phase of CuO (JCPDS # 48-1548) and hexagonal wurtzite phase of ZnO. No secondary phases were detected. The XRD peaks of ZnO in the CuO/ZnO samples became narrower with higher intensities owing to the heat treatment.

Fig. 4 shows the high-resolution TEM images with an energy dispersive X-ray (EDX) line profile of the CuO/ZnO structure. As shown in Fig. 4(b), elliptical-shaped CuO nanoparticles had an average size approximately ~30–40 nm, which were well distributed on the surfaces of the ZnO flowers, as shown in Fig. 4(a). A higher magnified image of the CuO/ZnO structure in Fig. 4(c) clearly revealed the growth of the CuO NPs on the ZnO flower and the interface between

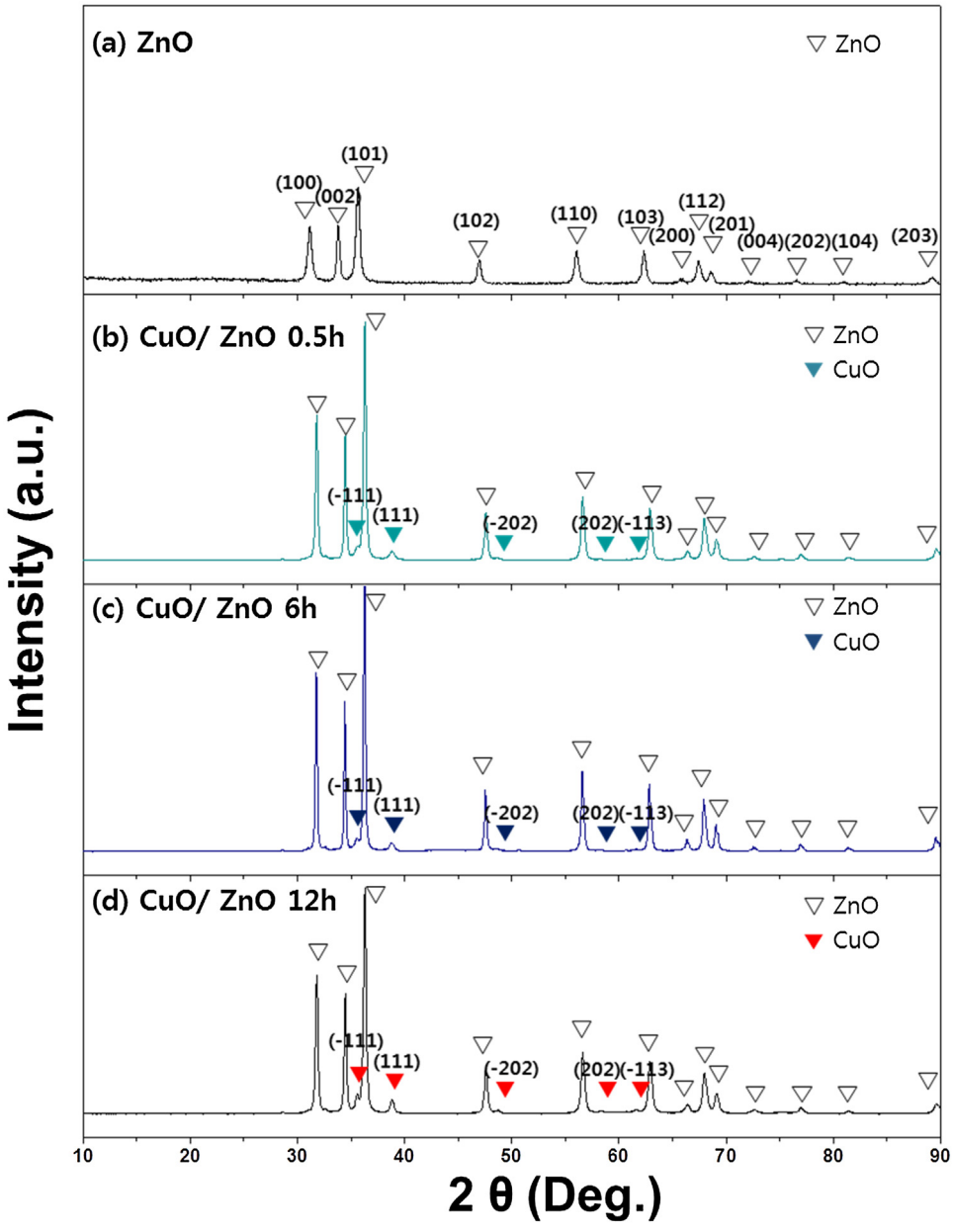

Fig. 3. Powder X-ray diffraction (PXRD) patterns of ZnO (empty triangles) and CuO/ZnO (filled triangles) samples with different ZnO synthesis times of 0.5, 6, and 12 h.

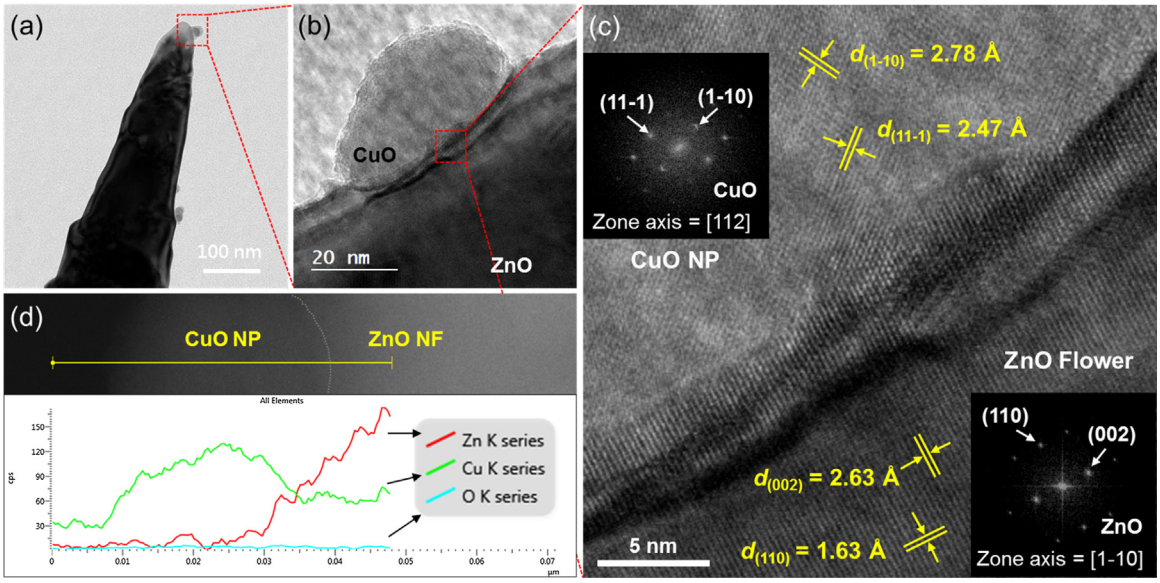

Fig. 4. (a) Transmission electron microscopy (TEM) image, (b) magnified TEM image, (c) more magnified TEM image with selected area diffraction patterns (SEAD), and (d) the high-resolution TEM images with energy dispersive X-ray (EDX) line profile of the CuO NPs/ZnO structures.

CuO and ZnO could be easily identified based on their differences in contrast. The lattice spacing of 1.63 and 2.63 Å for the ZnO flowers correspond to (110) and (002) planes of the wurzite ZnO. The CuO NPs also exhibit d-spacing values of 2.78 and 2.47 Å nm between two lattice fringes corresponding to the (1–10) and (11–1) planes of the CuO phase, as shown corresponding selected area diffraction patterns (SEAD) in the inset. The EDX scan profile in Fig. 4(d) confirmed the identity of Zn and Cu as well as a distinct interface between the two with no intermixing. The above results along with the XRD analysis strongly indicate that CuO/ZnO heterojunction structure.

3.2. Sensing properties of znO- and cuO/ZnO-based sensors

Fig. 5 presents the DMMP gas sensing properties of ZnO- and CuO/ZnO-based sensors with various synthesis times and at different operating temperatures of 300–400 °C. The corresponding resistances of the ZnO- and CuO/ZnO- based sensors in 10 ppm of DMMP are compared in Fig. 5(a) and (b). An example of the corresponding resistance in Fig. 5(a) showed that the resistance in air (R_a) of the CuO/ZnO based sensor increased due to the addition of CuO NPs on ZnO. The increased resistance (R_a) can be attributed to the higher surface area of the semiconductor that extends its depletion layer by forming *p*-CuO/*n*-ZnO junctions [29,30]. Further adsorption kinetic reactions occur between $C_3H_9O_3P$ and O^{2-} from the CuO NPs after exposure to DMMP, thus enhancing the corresponding response. During response/recovery cycles, as shown in Fig. 5(b), the resistance (R_g) and response times of the CuO/ZnO-based sensor significantly decreased (26.2 s) after exposure to DMMP compared to the ZnO based sensor (330 s)—an overall reduction by a factor of 13 for the CuO/ZnO-based sensors. We compare the sensing response of CuO, ZnO, and CuO/ZnO flower structures for DMMP detection. As shown in Fig. 5(c), the response of the CuO based sensor exhibited low responses in the range 1.1–2.1 in 10 ppm of DMMP at the operating temperature of 300–400 °C, which is ~20 times lower than ZnO based sensor. However the CuO/ZnO based sensor with 0.5 h synthesis of ZnO showed the highest response of 626.21 at 350 °C, indicating that significantly enhanced sensing properties are attributed to a synergetic effect of the *p*-CuO/*n*-ZnO junction structure. It also shows that the overall response in CuO/ZnO based sensor decreased with increasing the synthesis time of ZnO. Fig. 5(d) shows an overview of the dynamic sensing responses of the CuO/ZnO-based sensors as a function of DMMP concentration. The measured response of the CuO/ZnO-based sensor with a 0.5 h synthesis time is proportional to the DMMP concentration. The capability of the best performing sensor to selectively sense DMMP was evaluated alongside several gases, including NH_3, CO, NO, and NO_2, all at the same concentration (10 ppm) at 350 °C, as shown in Fig. 5(e). The response to DMMP exhibited the highest selectivity compared to other gases reaching a value of 626.21 at 350 °C.

The possible mechanism behind DMMP gas detection by *p*-CuO/*n*-ZnO heterojunction structures is displayed in Fig. 6. As shown in Fig. 6(a) and as observed in our results, the CuO NPs are randomly deposited on the surface of the ZnO flowers. With addition of the CuO NPs to the ZnO flowers, the p/n heterojunction was formed at the interface between p-type CuO NPs and ZnO flowers. While both CuO and ZnO are connected electronically in air, carriers (hole in CuO and electron in ZnO) will go through the opposite direction. For example, electrons transfer *n*-ZnO to *p*-CuO while holes go through *p*-CuO to *n*-ZnO until establishment of uniform fermi level in system, which leads to band bending in the depletion layer (Fig. 6(b)). When CuO/ZnO flowers are exposed to air, oxygen molecules are adsorbed on surface of ZnO with capturing the electrons in conduction band in ZnO, thus the resistance of the CuO/ZnO is increased further due to an additional depletion layer in PN junction, as described in Fig. 6(c). However, when CuO/ZnO flowers are exposed to DMMP, electrons were released by the gas sensing reaction between $C_3H_9O_3P$ and negatively charged surface oxygen (O^{2-}) on the conduction band of ZnO. The reductive DMMP molecules combine with holes in CuO, produce the intermediate, and then react with oxygen ions on the surface of ZnO, resulting in a decrease of the depletion layer and resistance [30]. Consequently, this allows for a highly sensitive detection of DMMP through a decrease of the resistance, hence the contribution of the sensing response from p-type CuO NPs is a predominant factor in the CuO/ZnO sensor, with the specific surface area of ZnO playing a critical role in improving the gas sensing properties.

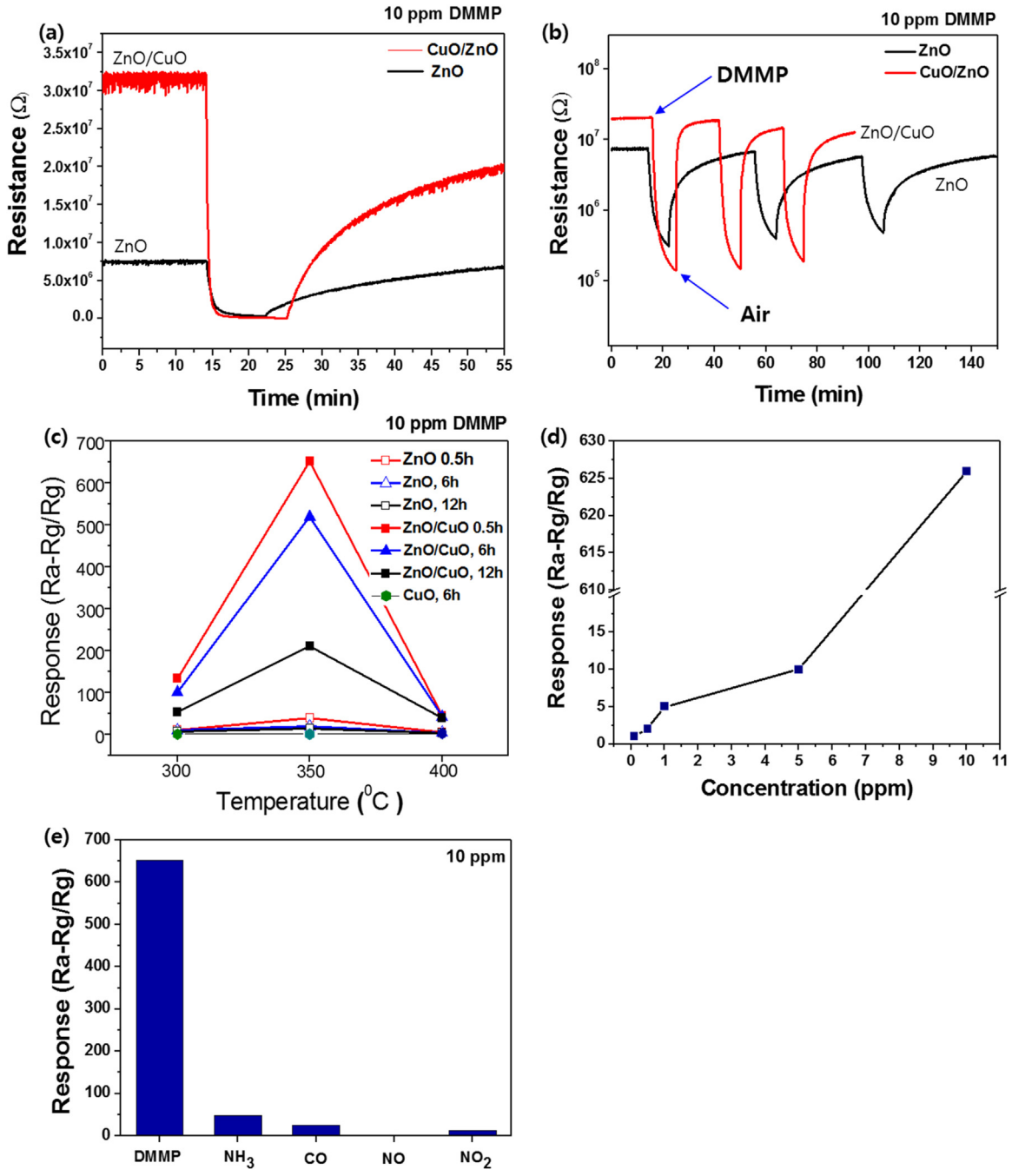

Fig. 5. (a) First response/recovery cycle and (b) repeatable response/recovery cycles of ZnO and CuO NPs/ZnO based sensors in 10 ppm dimethyl methylphosphonate (DMMP) at 350 °C, (c) response of CuO, ZnO, and CuO NPs/ZnO based sensors with various synthesis times (0.5, 6, and 12 h) at different operating temperatures of 300 400 °C, (d) dynamic response of the CuO NPs/ZnO based sensor to different concentrations of DMMP at 350 °C in air, and (e) selectivity of the CuO NPs/ZnO based sensor to other gases of NH_3, CO, NO, and NO_2 at the same concentration (10 ppm) at 350 °C.

4. Conclusions

We demonstrated a hydrothermal method for fabricating CuO NPs on high surface area ZnO flowers, which have highly sensitive DMMP gas sensing capabilities. PXRD and TEM analyses confirm the formation of CuO/ZnO heterojunction structures. The BET surface areas of the *p*-CuO/*n*-ZnO samples decreased with increasing the synthesis times of ZnO. The gas sensing properties showed that the response time of the CuO/ZnO heterojunction sensor decreased to 26.2 s after exposure to DMMP compared to the ZnO based sensor (330 s). The heterojunction structures' responses to DMMP exhibited the highest selectivity compared to other gases, reaching a value of 626.21 at 350 °C. The formation of CuO NPs and ZnO heterojunction structure indicates that an increase of the depletion layer and the structures' resistance (R_a) in air, leading to a decrease of the depletion layer and resistance when exposed to reducing DMMP gas. In addition, the higher surface area (6.0 m^2/g) of the CuO/ZnO heterojunction structure with a 0.5 h synthesis time of the ZnO flowers supported further adsorption kinetic reactions between $C_3H_9O_3P$ and O^{2-} ions after exposure to DMMP, thus enhancing the corresponding response.

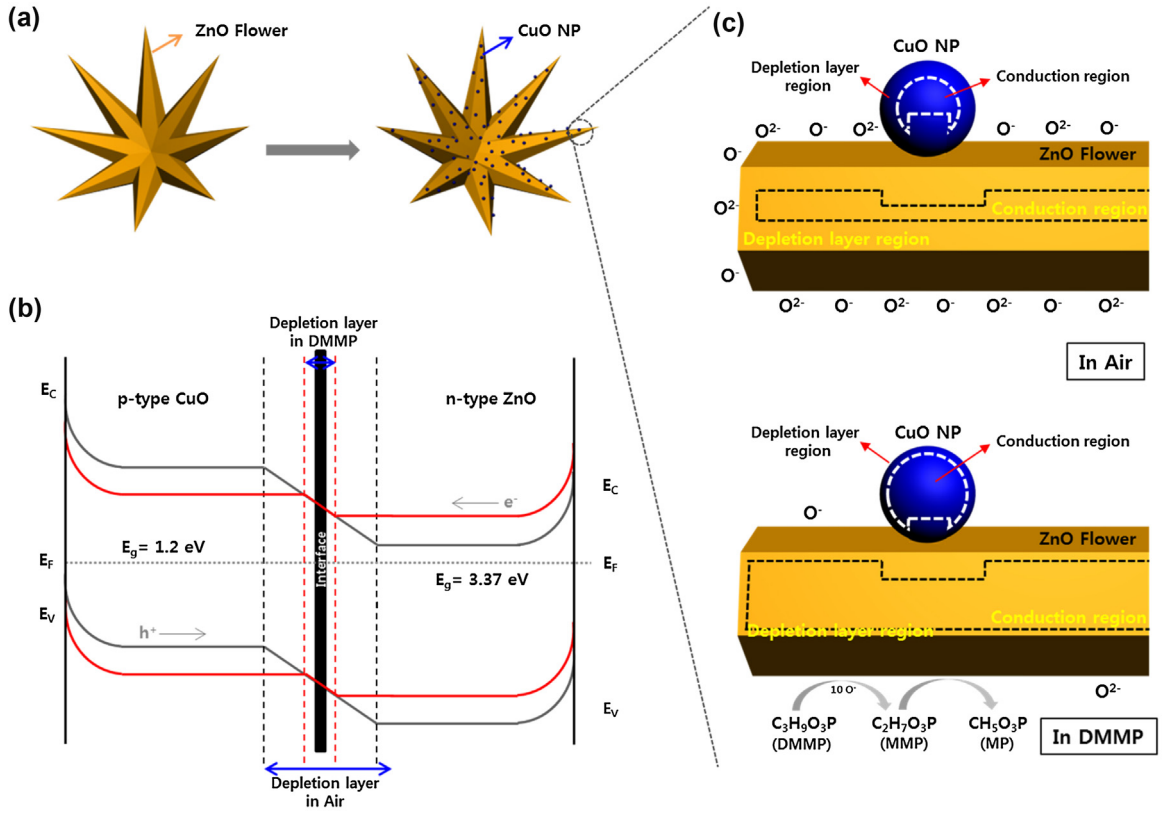

Fig. 6. Schematic diagram of (a) CuO NPs deposited on the surface of ZnO flowers, (b) the energy band gap of a CuO/ZnO *p-n* junction, and (c) the sensing mechanism of the CuO NPs/ZnO sensor in air and in DMMP. When the sensor exposed to reducing gas (DMMP), the surface adsorption occurred by the gas sensing reaction between $C_3H_9O_3P$ and negatively charged surface oxygen (O^{2-}), leading to a decrease of the depletion layer and resistance.

Acknowledgment

This work was supported by the Agency for Defense Development (ADD) of the Republic of Korea and Korea Ministry of Environment as "Convergence Technology Program (2015001650001)" and Priority Research Centers Program (2009-0093823) through the National Research Foundation of Korea (NRF).

References

[1] F. Worek, M. Koller, H. Thiermann, L. Szinicz, Toxicology 214 (2005) 182–189.
[2] N.J. Choi, Y.S. Lee, J.H.A. Kwak, J.S. Park, K.B. Park, K.S. Shin, H.D. Park, J.C. Kim, J.S. Huh, D.D. Lee, Sens. Actuators B 108 (2005) 177–183.
[3] E. Brunol, F. Berger, M. Fromm, R. Planade, Sens. Actuators B 120 (2006) 35–41.
[4] Z. Ying, Y. Jiang, X. Du, G. Xie, J. Yu, H. Wang, Sens. Actuators B 125 (2007) 167–172.
[5] E. Comini, G. Faglia, G. Sberveglieri, Z.W. Pan, Z.L. Wang, Appl. Phys. Lett. 81 (2002) 1869–1871.
[6] H.-C. Kim, S.-H. Hong, S.-J. Kim, J.-H. Lee, J. Sens. Sci. Technol. 20 (2011) 294–299.
[7] Y. Yang, H.-F. Ji, T. Thundat, J. Am. Chem. Soc. 125 (2003) 1124–1125.
[8] G. Zuo, X. Li, P. Li, T. Yang, Y. Wang, Z. Cheng, S. Feng, Anal. Chim. Acta 580 (2006) 123–127.
[9] X. Du, Z. Wang, J. Huang, S. Tao, X. Tang, Y. Jiang, J. Mater. Sci. 44 (2009) 5872–5876.
[10] Y. Zhao, J. He, M. Yang, S. Gao, G. Zuo, C. Yan, Z. Cheng, Anal. Chim. Acta 654 (2009) 120–126.
[11] X. Du, Z. Ying, Y. Jiang, Z. Liu, T. Yang, G. Xie, Sens. Actuators B 134 (2008) 409–413.
[12] W. Wang, S. He, S. Li, Y. Pan, Smart Mater. Struct. 15 (2006) 1525–1530.
[13] M. Gardon, J.M. Guilemany, J. Mater. Sci. Mater. Electron. 24 (2013) 1410–1421.
[14] P. Xu, Z. Cheng, Q. Pan, J. Xu, Q. Xiang, W. Yu, Y. Chu, Sens. Actuators B 130 (2008) 802–808.
[15] A. Khanna, R. Kumar, S.S. Bhatti, Appl. Phys. Lett. 82 (2003) 4388–4390.
[16] D. Barreca, D. Bekermann, E. Comini, A. Devi, R.A. Fischer, A. Gasparotto, C. Maccato, G. Sberveglieri, E. Tondello, Sens. Actuators B 149 (2010) 1–7.
[17] Y.-H. Ho, W.-S. Huang, H.-C. Chang, P.-K. Wei, H.-J. Sheen, W.-C. Tian, Appl. Phys. Lett. 106 (2015) (183103-183103-4).
[18] Y.B. Zhang, J. Yin, L. Li, L.X. Zhang, L.J. Bie, Sens. Actuators B 202 (2014) 500–507.
[19] D. Barreca, E. Comini, A. Gasparotto, C. Maccato, C. Sada, G. Sberveglieri, E. Tondello, Sens. Actuators B 141 (2009) 270–275.
[20] Y.-S. Kim, I.-S. Hwang, S.-J. Kim, C.-Y. Lee, J.-H. Lee, Sens. Actuators B 135 (2008) 298–303.
[21] M.L. Zhong, D.C. Zeng, Z.W. Liu, H.Y. Yu, X.C. Zhong, W.Q. Qiu, Acta Mater. 58 (2010) 5926–5932.
[22] I.-S. Hwang, J.-K. Choi, S.-J. Kim, K.-Y. Dong, J.-H. Kwon, B.-K. Ju, J.-H. Lee, Sens. Actuators B 142 (2009) 105–110.
[23] H. Bae, G. Choi, Sens. Actuators B 55 (1999) 47–54.
[24] J.D. Choi, G.M. Choi, Sens. Actuators B 69 (2000) 120–126.
[25] C.S. Dandeneau, Y.-H. Jeon, C.T. Shelton, T.K. Plant, D.P. Cann, B.J. Gibbons, Thin Solid Films 517 (2009) 4448–4454.
[26] S.-J. Jung, H. Yanagida, Sens. Actuators B 37 (1996) 55–60.
[27] J.X. Wang, X.W. Sun, Y. Yang, K.K.A. Kyaw, X.Y. Huang, J.Z. Yin, J. Wei, H.V. Demir, Nanotechnology 22 (2011) 325704 (7pp).
[28] N. Wu, M. Zhao, J. Zheng, C. Jiang, B. Myers, S. Li, M. Chyu, S.X. Mao, Nanotechnology 16 (2005) 2878–2881.
[29] Y.-B. Zhanga, J. LingLi, L.-X. Zhanga, L.-J. Bie, Sens. Actuators B 202 (2014) 500–507.
[30] Q. Simon, D. Barreca, A. Gasparotto, C. Maccato, E. Tondello, C. Sada, E. Comini, G. Sberveglieri, M. Banerjee, K. Xu, A. Devi, R.A. Fischer, Chem. Phys. Chem. 13 (2012) 2342–2348.
[31] A. Katoch, S.-W. Choi, J.-H. Kim, J.H. Lee, J.-S. Lee, S.S. Kim, Sens. Actuators B 214 (2015) 111–116.
[32] B. Cai, Y. Zhou, M. Zhao, H. Cai, Z. Ye, L. Wang, J. Huang, Appl. Phys. A 118 (2015) 989–996.
[33] R. Yoo, J. Kim, M.-J. Song, W. Lee, J.S. Noh, Sens. Actuators B 209 (2015) 444–448.
[34] R. Yoo, S. Cho, M.-J. Song, W. Lee, Sens. Actuators B 221 (2015) 217–223.

Biographies

Ran Yoo earned her Master's Degree in Materials Science and Engineering at Yonsei University in 2013. She is currently studying on the nerve agent gas sensor using carbon nanotubes or metal oxide toward her Ph.D in Nerve Agent Gas sensor at Yonsei University.

Somi Yoo earned her Bachelor's Degree in 2014. Her current research interests include thermoelectric transport properties of low-dimensional materials and gas sensors based on nano-materials in Materials Science and Engineering at Yonsei University.

Dongmei Lee earned her Bachelor's Degree in Biology Engineering at YanBian University in 2014. She is currently studying on the nerve agent gas sensor using metal oxide toward her MS in Nerve Agent Gas sensor in Materials Science and Engineering at Yonsei University.

Jeongmin Kim obtained his BS degree in metallurgical engineering from the Yonsei University (Korea) in 2008. He earned Ph.D. degree in Materials Science and Engineering at the Yonsei University in 2016. His current research interests include Galvano-magnetic and thermoelectric transport properties of low-dimensional materials and gas sensors based on nano-materials.

Sungmee Cho earned her Ph.D. degree in Electrical & Computer Engineering from Texas A&M University in 2011. She was a postdoc researcher in Materials Science and Engineering at Northwestern University in 2011–2012. She has been with Doosan Corporation as a researcher in 2003–2004 and Korea Institute Science Engineering (KIST) as a researcher in 2002–2003 and 2004–2005. Now she is a research professor in Creative Materials Division for BK21 PLUS program of Yonsei University. Her current research interests include Mg_2Si-based thermoelectric (TE) energy conversion, TE module joint, thin film hydrogen storage, hydrogen gas, solid oxide fuel cell (SOFC), and Li ion battery.

Wooyoung Lee is a professor of Department of Materials Science and Engineering, the chairman of Yonsei Institute of Convergence Technology and the Head of Institute of Nanoscience and Nanotechnology at Yonsei University in Korea. He received a BS degree in Metallurgical Engineering in 1986, a MS degree in Metallurgical Engineering from the Yonsei University in 1988. He received a Ph.D. degree in Physics from University of Cambridge, England in 2000. He is also the director in Korea-Israel Industrial R&D Foundation and the advisor in National Assembly Research Service. In recent years, his research interests have centered on spintronics, thermoelectric materials and devices, hydrogen sensor, hydrogen gas storage, various gas sensors, rare earth and non-rare earth permanent magnets. He has received a number of awards in nano-related research areas and a Service Merit Medal (2008) from the Korean Governments due to contribution on the development of intellectual properties. He has authored and co-authored over 150 publications, and has edited a few of special books on nano-structured materials and devices.